VARIATIONS IN PHYSICAL PROPERTIES WITHIN THE EARTH'S CRUSTAL LAYERS.

BENO GUTENBERG.

ABSTRACT. In two recent papers (Gutenberg, 1943a, 1944b) the author has investigated with as high an accuracy as practicable travel times and average wave velocities in the crustal layers in southern California. However, it is not possible to use the observed time data for conclusions as to the changes of the velocity within a given layer; the expected effects are of the same order of magnitude as the effects of local differences in structure (Gutenberg, 1943c). Zoeppritz (1912) was the first to point out that changes with distance in the amplitudes of the observed waves may give information of this kind. The method outlined by him is employed in the present paper to study the changes in the velocity of elastic waves, the bulk modulus and the coefficient of rigidity with depth within the layers of the earth's crust. The results are compared with data found from laboratory experiments. The depth at which the melting point is reached is discussed.

CONTENTS.

MATERIALS USED.

THE first part of the paper is based on original seismograms of 50 southern California earthquakes recorded at the Pasadena group of 8 stations, at 5 stations of the Berkeley group (courtesy of Dr. P. Byerly), at the 4 stations of the Lake Mead group (courtesy of the Bureau of Reclamation, National Park Service, and the U. S. Coast and Geodetic Survey) and at Tucson (courtesy of the U. S. Coast and Geodetic Survey). For detailed data on the shocks and stations, see Gutenberg (1943a).

All records available for these shocks were measured for time data, but only records of standard Wood-Anderson torsion

seismographs ($V=2800$, $T_0=0.8$ sec., $h=0.8\pm$) were used for measurements of amplitudes. The dynamic magnification of these instruments changes very little; and in addition corrections (including the effect of ground) to reduce recorded amplitudes to a standard average have been determined for all instruments of this type at the stations mentioned (Gutenberg, 1943a, Table 5). Records of other instruments can be used only when the instrumental constants are known sufficiently well for the time of any given shock. This requirement practically eliminates instruments with electromagnetic recording for the present purpose (although their high magnification renders them unsurpassed for the study of time data) for their free periods and their static magnifications as well depend on the width of air gaps or distances between coils and magnets, which change with temperature. Consequently, no vertical-component records were available for use in the first part of this paper. The amplitudes in mm, of longitudinal waves measured on the NS- and EW-components of the standard torsion seismographs were combined to determine the amplitude of the horizontal component, and the logarithm of this amplitude was taken; then the above mentioned correction for the particular station was subtracted, as well as the quantity M-5; M is the magnitude of the shock, as defined by Richter (1935) and determined for the 50 shocks by Gutenberg (1943a, Table 3). This gives approximately the logarithm of the average amplitude (in mm) of longitudinal waves which would be recorded in southern California by a standard torsion seismograph along the direction toward the epicenter for a shock of magnitude 5. The results found in this way form the basic material for Table I.

The records available from the 50 shocks cover practically the whole range within which $\bar{P}$ and Py can be identified. (For symbols, see Fig. 1)[1] However, only a few records are available for distances beyond 500 km, so that additional shocks must be used to investigate Pn at greater distances and to obtain data for depths below about 70 km. Some records of the Pasadena group of stations covering distances between 9° and 29° have already been discussed by Gutenberg and Richter (1931). For additional information, Gutenberg and Richter (1939) have studied records of shocks originating near and recorded at Huancayo, Peru from 1933 to July, 1937.

[1] Figures in this paper were drafted by Mr. J. M. Nordquist.

Records of this station (two horizontal Wenner and one long period vertical Benioff seismographs) are now on file at Pasa-

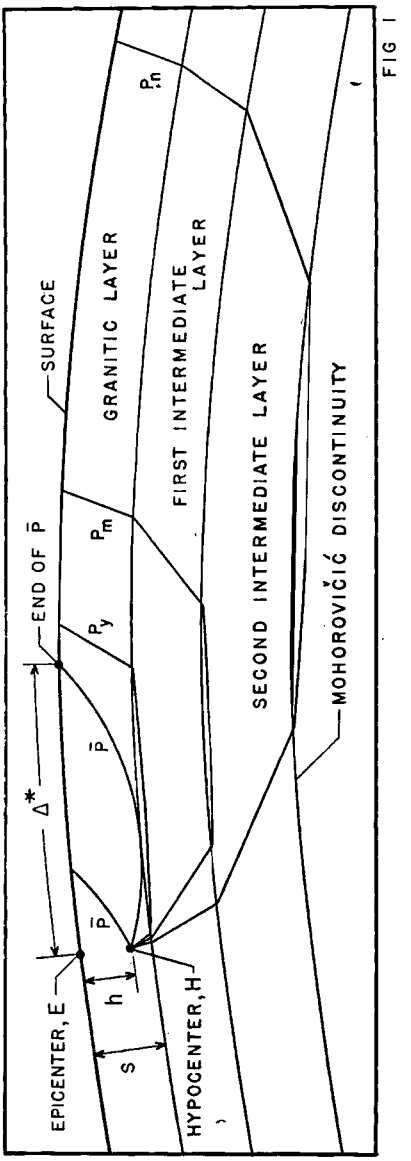

dena up to December, 1942 (courtesy of the Carnegie Institution of Washington). Focal depths and epicentral distances of shocks with records suitable for the present purpose were

determined for additional shocks (Table VIII). Huancayo is one of the very few stations with sufficiently sensitive instruments which is favorably located with respect to the belts of intermediate and deep shocks to furnish the information desirable here.

OBSERVATIONS OF AMPLITUDES OF LONGITUDINAL WAVES AT SHORT DISTANCES.

The determination of horizontal amplitudes as described in the preceding section is affected by several sources of errors. First, our method of calculation supposes that the trace amplitudes of the longitudinal waves (symbol P) on the standard torsion seismographs increase with the magnitude proportional to the trace amplitudes in the S-group (transverse waves) at the distances used in the present paper, as the latter are used in the determination of the magnitude. No large errors are to be expected from this assumption as in the large majority of the records used the range of magnitude was less than 1½ units. The observations indicate that in 6 shocks originating near the Inglewood fault the logarithm of S/P was between 1.0 and 1.2 using all stations, but was 0.6±0.2 in most other shocks. The rather large values in the former are at least partly the result of the fact, that several stations are close to a "nodal line" for the P-waves (Gutenberg, 1941; see also next paragraph). In some other instances, Pn was unusually small; this is true for most shocks in Imperial Valley, as recorded at Pasadena and Mt. Wilson, and is probably due to effects of deep sediments or mountain roots along the path of the waves.

Second, the theory assumes that for a given phase the energy is radiated equally in all directions from the source. This is not correct (see Gutenberg, 1941, Figs. 1 and 2). Fortunately, the resulting amplitudes are too small by one half or more (or the logarithm by 0.3 or more) in a small range of directions only. No attempt has been made to correct for this effect, as the direction of faulting is not known accurately enough.

Table I contains logarithms of average amplitudes, usually for distance ranges of 10 km., but covering longer intervals where data were scanty. It is based on the observations described in the preceding section.

GENERAL THEORY.

The method of Zoeppritz (1912) leads to the following equation for the horizontal amplitudes u of longitudinal (and

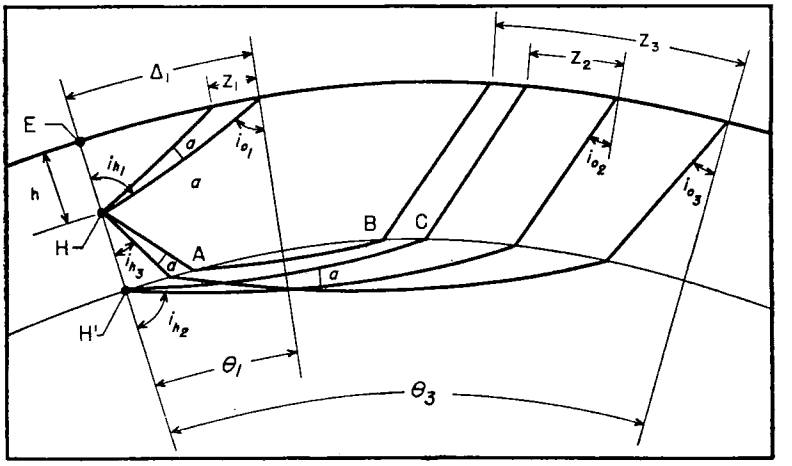

FIG. 2

similarly of transverse) waves arriving at an epicentral distance Δ in km. from a source at a depth h (hypocenter H, Fig. 2)

$$u = C\left(\frac{u}{A}\right)_0 \sqrt{\frac{FK \sin i_h \frac{di_h}{d\Delta}}{\Delta \cos i_0}} \quad \ldots\ldots\ldots\ldots (1)$$

C = constant, depending on the energy of the shock and the period at the point of observation; the latter is assumed to be constant but it really increases slightly with distance. $(u/A)_0$ = ratio of the horizontal component of the ground displacement to the incident wave amplitude taken at the station. It depends on Poisson's ration and on i_0, the angle of incidence at the surface. For characteristic values see Table X.

F is to be used if the wave under consideration is refracted (or reflected) at a discontinuity (at A, B, C in Fig. 2). It gives the fraction of energy which passes through the discontinuity in a refracted wave or is reflected into a reflected wave. In case of several refractions or reflections or both the product of such factors is to be taken. A summary of the theory and of values of F calculated under various assumptions has been given by the author after completion of the present paper (Gutenberg, 1944a).

TABLE I.

Average amplitudes of longitudinal waves in southern California as a function of distance, for shock of magnitude 5.0. The figures given are the logarithms of the horizontal amplitudes in mm., as they would be recorded by a standard torsion Wood-Anderson seismograph (static magnification 2800, free period 0.8 seconds, damping factor $h = 0.8$ to 0.9). a) 43 shocks in southern California, b) 7 shocks in northern Owens Valley. n = number of records.

	Logarithm of Amplitudes							
Distance	$\bar{P}$		Py		Pn		n	
km.	a)	b)	a)	b)	a)	b)	a)	b)
1-9	2.5						2	
20-29	2.1						3	
30-39	2.1						7	
40-49	1.3						7	
50-59	1.5						6	
60-69	1.4						3	
70-79	1.1	1.0					12	6
80-89	1.0						10	
90-99	1.1		0.5				15	
100-109	1.3		0.6				7	
110-119	1.2		0.4				7	
120-129	1.3		0.6				4	
130-139	0.8		0.2		−0.2		8	
140-149	1.2		0.8		0.3		5	
150-159	0.9		0.6		0.0		9	
160-169	1.0		0.8		0.3		23	
170-179	1.1	1.2	1.0	0.8	0.3		17	7
180-189	1.1		1.0		0.3		7	
190-199	1.0		1.0		0.1		3	
200-209	0.4		0.5				4	
210-219	0.8		0.6		−0.1		6	
220-229	0.5		0.4		−0.4		6	
230-249	0.6		0.3		−0.3		10	
250-259	0.7		0.9		−0.1		8	
254-264		0.6		0.5		−0.2		5
260-269	0.6		0.5		−0.5		6	
270-279	0.7		0.2		−0.6		15	
280-299	0.4		0.0		−1.0		5	
300-309		0.5		0.2		0.0		6
310-319	0.6	0.2	0.4	0.0	−0.6	−0.3	8	6
320-329	0.5		0.0		−0.5		7	
330-349	0.2		0.0		−0.2		3	
350-359	0.2	−0.1	0.0	−0.4	−0.1	−1.4	6	5
360-369	0.1	0.1	−0.1	−0.4	−0.8	−0.8	6	2
370-379	0.2	0.0	−0.0	−0.2	−0.6	−1.3	9	6

TABLE I—(Continued).

Distance km.	$\bar{P}$ a)	$\bar{P}$ b)	Py a)	Py b)	Pn a)	Pn b)	n a)	n b)
	Logarithm of Amplitudes							
380-389	0.2	0.3	0.0	0.3	−0.4	−1.0	3	8
390-399	−0.1	0.1	−0.3	0.0	−0.5	−1.4	5	4
400-415	0.0	0.1	−0.2	−0.1	−0.6	−0.8	7	5
426-441	−0.2		0.0		−0.8		6	
448-457	−0.3		−0.4		−0.9			
473-486	−0.3		−0.4	−0.4	−0.9	−1.4	3	6
531-552	−0.5		−0.6		−1.4		3	
560-576	−0.5				−1.2		2	
680-682					−0.8		2	
700-800					(−2±)		5	

In equation (1), K gives the effect of the absorption. For body waves, the average value of the absorption factor is about 0.00012 per km. (from unpublished results of the author). Consequently, their amplitudes are reduced by less than 5 per cent over the range of distances used in the present paper, so that K can be neglected.

Finally, equation (1) contains the angle of incidence at the source, i_h, its derivative with respect to the distance Δ, this distance itself and the angle of incidence at the station, i_o. Of these, the value of $di_h/d\Delta$ is the most important. It is inversely proportional to the width Z (Fig. 2) of the zone which is formed by a pair of rays forming the constant angle a at the source. Its large variations may be seen from the various cases sketched in Fig. 2. Its functional relationship to Δ and i_o is treated separately for $\bar{P}$, *Py* and *Pn* in the following sections.

In studying gradual changes of velocity V with depth, h, it is convenient to assume that the increase of V is proportional to h,

$$V_h = V_o + bh \quad \ldots\ldots\ldots\ldots\ldots\ldots (2)$$

$$dV_h/dr = -b \quad \ldots\ldots\ldots\ldots\ldots\ldots (3)$$

Throughout this paper h is measured in km. $h = R - r$, R = radius of the earth, r = radius of the sphere at the depth h. The subscript $_o$ refers to the surface of the earth. If equation (3)

holds, all rays are parts of circles with the radius ρ_h, given by

$$\rho_h = \frac{V_h}{\left(\frac{dV}{dr}\right)_h \sin i_h} = -\frac{V_h}{b \sin i_h} = -\frac{V_o}{b \sin i_o}\,\frac{r}{R} \quad \ldots\ldots(4)$$

In particular, using equation (4), if $i_h = 90°$, we find $\rho_h{}^*$

$$\rho_h{}^* = -\frac{V_h}{b} \qquad \rho_h \sin i_h = \rho_h{}^* = \text{constant.} \quad \ldots\ldots(5)$$

The velocity V of longitudinal waves, v of transverse waves, the bulk modulus k, the density d and Poisson's ratio σ are connected by the following equations:

$$k = d\,(V^2 - \tfrac{4}{3}v^2) = dV^2\frac{1+\sigma}{3(1-\sigma)} \quad \ldots\ldots(6)$$

$$\sigma = 0.5\left[1 - \frac{1}{(V/v)^2 - 1}\right] = \frac{0.5\,(V/v)^2 - 1}{(V/v)^2 - 1} \quad \ldots\ldots(7)$$

If the change in density with depth is due only to a change Δp of the pressure p and not to a change in material, and the compression involved is adiabatic, then we have approximately in a relatively thin layer of a given material

$\Delta d/d = \Delta p/k$ and

$$\frac{V+\Delta V}{V} = \sqrt{\frac{k+\Delta k}{k}\,\frac{d}{d+\Delta d}} = \text{approx.}\left(1 + \frac{\Delta k - \Delta p}{2k}\right) \quad \ldots\ldots(8)$$

$$\frac{\Delta V}{V} = \frac{\Delta k - \Delta p}{2k} \qquad \frac{\Delta k}{k} = \frac{2\Delta V}{V} + \frac{\Delta p}{k}, \text{ where } \Delta V = b\,\Delta h \quad \ldots(9)$$

If x is the change in k expressed in per cent for a change in pressure by 1000 atmospheres, which corresponds to a change in depth of about $\Delta h = 10/d$ km., and if k given in dynes per cm^2, then we have

$$x = \frac{200\,b\,\Delta h}{V} + \frac{10^{11}}{k} = \frac{2000\,b}{V\,d} + \frac{10^{11}}{k} \quad \ldots\ldots(10)$$

The effect on the density of the increase in temperature with depth has been studied by Birch (1939). He found that for a temperature gradient of several degrees per km., equations (8) may become seriously inadequate. However, as b can be found only approximately, the other quantities need not be known very accurately. For the calculations the values given in Table II have been used. For the values of V and v, see Gutenberg (1944b); d is assumed; k, μ and σ result from V, v and d.

In addition, the value of b in the various layers, must be known. Consequently, our next problem is, to find the change of velocity with depth in each of the crustal layers, which gives b.

TABLE II.

Average velocity V of longitudinal waves, bulk modulus k, density d and Poisson's ratio σ in Southern California.

	V(km./sec.)	v(km./sec.)	k(dynes/cm.²)	μ(dynes/cm.²)	d	σ
Granitic layer	5.58	3.26	4.6×10^{11}	2.9×10^{11}	2.7	0.24
First intermediate layer	6.03	3.64	5.4×10^{11}	3.8×10^{11}	2.9	0.21
Second intermediate layer	6.91	4.08	7.9×10^{11}	5.2×10^{11}	3.1	0.23
Below intermediate layers	8.00	4.40	12.6×10^{11}	6.4×10^{11}	3.3	0.28

THE CHANGE OF VELOCITY OF LONGITUDINAL WAVES WITH DEPTH IN THE GRANITIC LAYER.

The longitudinal wave through the uppermost layer (neglecting the sediments), the so called "granitic layer," has been

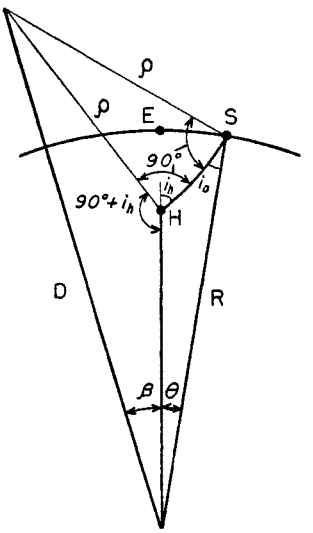

FIG. 3

given the symbol $\bar{P}$ (Fig. 1). To find the quantities under the square root in equation (1) we use Figure 3 and equation (5):

$$\left.\begin{aligned}\tan\beta &= \frac{\rho\cos i_h}{r+\rho\sin i_h} = \frac{\rho\cos i_h}{r+\rho^*}\\ \cos(\beta+\Theta) &= \frac{D^2+R^2-\rho^2}{2DR}\end{aligned}\right\} \quad \ldots\ldots\ldots\ldots\ldots\ldots\ldots\ldots (11)$$

$$D^2-\rho^2-r^2 = 2\rho r\sin i_h = 2\rho^* r;\ D^2+R^2-\rho^2 = 2\rho^* r+r^2+R^2 = \text{constant} \ldots (12)$$

$$D = \rho\cos i_h/\sin\beta \quad \ldots\ldots\ldots\ldots\ldots\ldots\ldots\ldots\ldots\ldots\ldots (13)$$

Equations (11) to (13) permit the finding of Θ as a function of i_h; i_o can be found from the ray equation

$$\frac{r\sin i_h}{V_h} = \frac{R\sin i_o}{V_o}. \quad \ldots\ldots\ldots\ldots\ldots (14)$$

$(d\cos i_h/d\Delta)$ can be found graphically, $F=1$, and equation (1) can be used in the calculation of u as a function of Δ, except for the constant factor C. In the calculations, $(d\cos i_h/d\Delta)$ was measured per 100 km. and the best agreement between the values of log u thus calculated and for the observations for a shock of magnitude 5 was found for log $C=2.0$. For straight rays (v and V constant, $b=0$) equation (1) may be written

$$u = C\left(\frac{u}{A}\right)_o \sqrt{\frac{\sin i_h}{\Delta(\cos i_o - \frac{r}{R}\cos i_h)}} \quad \ldots\ldots\ldots\ldots (15)$$

In order to compare the results found from equation (15) with those calculated for other values of b, $2-0.90=1.10$ must be added to the resulting values of log u as $(d\cos i_h/d\Delta)$ now is measured per radian. $(0.90=1/2\log 6370/100.)$

As long as b in equation (2) is within reasonable limits, the calculated curves for log u as a function of Δ differ mainly by the distance Δ^*, at which the direct waves end (See Fig. 1). For distances shorter than Δ^* the calculated values of log u are practically the same. Table III gives the observed values of log u (from Table I) and those calculated from (15) for log $C=1.10$. Up to $\Delta=325$ km., the agreement is very good. Beyond, the observed values are one-half of the calculated or less, indicating that very probably the end of the direct $\bar{P}$-waves occurs at a distance of about $\Delta^*=325$ km. Theoretically, the value of u is zero at the epicenter (the movement there is supposed to be purely vertical), and reaches its maximum at a distance of about 25 km. The two observed values near the

epicenter give log $u=2.5$. The difference is partly instrumental and partly due to the fact that the source is not a point.

TABLE III.

Observed and calculated values of log u for $\bar{P}$ in a shock of magnitude 5. Details as in Table I.

Δ in km.	25	50	100	150	200	250	300	325	350	400	500
obs.	2.1	1.5	1.2	1.0	0.7	0.6	0.5	0.5	0.1	0.0	−0.4
calc.	1.8	1.5	1.1	0.9	0.7	0.6	0.5	0.4	0.4	0.3	0.1

The value of Δ^* (Fig. 1) depends mainly on the depth of focus, h, the thickness, s, of the layer and the radius of curvature of the rays, given by b (supposed constant). If the first two quantities are known, b can be found. From travel time observations (Gutenberg, 1943a) as well as the amplitudes of Py (next section) it appears probable that the source H (Fig. 1) of at least a large majority of the earthquakes used was at the bottom of the granitic layer; consequently $h=s$. For the limiting ray (see Fig. 3) $\beta=0$, $D-R+\rho^*=h$, and equation (11) gives Θ^*, from which Δ^* can be found. Results for $h=s=$ 18 km., which may be in error by ± 3 km., are given in Table IV.

TABLE IV.

Corresponding values of b and Δ^*, if $h=s=18$ km. (Fig. 1).

b	0.0000	0.001	0.0013	0.002	0.0043	0.01
Δ^*	479	328	304	265	190	137 km

From Table III it seems likely that Δ^* is approximately 325 km.; Table IV then gives $b=0.001$. This is at least the order of magnitude of b; errors are introduced by effects of sedimentary layers, locally variable values of h and s, misinterpretation of $\bar{P}$ in seismograms and the assumption that the increase in velocity is proportional to h. In granitic material the velocity increases much more rapidly in the uppermost kilometer than at larger depth (Birch et al., 1942, p. 97). This increase depends on the age of the granite, the depth at which it was formed, the thickness of overlying sediments, and the composition.

With $b=0.001$, equation (10) shows that the bulk modulus k would increase by about ½ per cent with an increase of depth

corresponding to an increase of pressure p by 1000 atm. For small strains, Birch (1938) found theoretically that approximately $\delta(1/k)/\delta p = -5/k^2$. This gives for the first two layers an increase in k of the order of magnitude of 1 per cent, if p increases by 1000 atm. Laboratory experiments of Adams and Williamson (1923; see also Birch et al., 1942, p. 62) gave a bulk modulus of about 5×10^{11} dynes per cm.^{2} at a pressure of 5000 atm. in agreement with the value found from seismic data (Table II), and an increase by about 2 per cent corresponding to an increase of pressure by 1000 atm. However, these results did not consider the effect of temperature. Findings of Birch (1943) indicate that this reduces the effect of pressure by at least one half. Birch and Dow (1936) calculated the compressibility as a function of depth for a diabase, including the temperature effect. This reduced the increase in bulk modulus with depth by about ½ as compared with the assumption of a constant temperature. In all instances, the increase of k with pressure was much greater for the first 1000 atm. than for specimens already under a pressure of a few thousand atm. at the beginning of the experiments. The results from seismic velocity data show the same phenomenon. Apparently, in the uppermost km. b is roughly 0.1 or even larger (Birch et al., 1942, p. 97), which gives an increase in k by at least 15 per cent for the first 1000 atm. Except for the uppermost 1 or 2 km. where the velocity is relatively low, the assumption of a velocity $V = 5.56 + 0.001\ h$ km./sec (h = depth in km.) for longitudinal waves in the granitic layer explains all the observations. Improvements would consist in a more accurate determination of the factor b and in assuming a better functional relationship between V and h.

THEORY AND OBSERVATIONS FOR *Py* AND *Pm*.

Unlike P̄, the *Py* waves having their deepest point in the first intermediate layer (Fig. 1) have definitely different velocities depending on the region (Gutenberg, 1943b). There may be one or several intermediate layers. In the present paper we use the symbol *Py* for the wave through the first intermediate layer. In European earthquakes the symbol *P** is used for a similar wave with a different velocity

The equations for the calculation of the amplitudes depend on whether the source is within the granitic layer (*H* in Fig. 2)

or at its bottom (H'). In the first case much smaller amplitudes are to be expected than in the second. The ratio p of the calculated amplitude in the first case over that in the second is given approximately by

$$p = 0.2 \sqrt{f\,(90° - i_2)} \quad \ldots\ldots\ldots\ldots\ldots\ldots (16)$$

where f = fraction of energy refracted into the intermediate layer, and i_2 = angle of incidence in the intermediate layer in degrees. f increases from zero for $i_2 = 90°$ to about 0.7 for $i_2 = 87.5°$; $i_2 = 89°$ corresponds to an epicentral distance

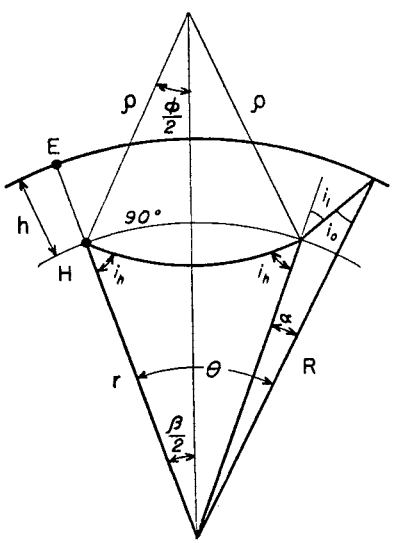

FIG. 4

usually between 100 and 200 km., depending on the value of b. Thus, p is smaller than 0.1 at the distances where Py begins to precede $\bar{P}$ and to be observable.

The chief difficulty in the calculation of Py and Pn arises from the fact that the equations used in general for the calculation of the energy of reflected and refracted waves does not hold for waves traveling in the high velocity layer almost parallel to the boundary (angle of incidence greater than about 85°). The strain set up in the low velocity layer by such waves arriving earlier than those on the low velocity side of the boundary produces an energy flow across the boundary from the side of high velocity to that of low velocity. This phenomenon was first recognized from observations; the refracted

waves were found to be by far larger than calculations indicated (Schmidt, 1938, 1939). The observations were explained qualitatively by Joos and Teltow (1939) and Ott (1942). We must, therefore, expect that Py and Pn are noticeably larger at short distances than the classical theory would indicate and somewhat smaller at long distances.

We assume now that *Py* is in the boundary (*H'* in Fig. 2). From Fig. 4 we find with sufficient approximation

$$\Theta = a + \beta \qquad a = i_1 - i_c \qquad \ldots\ldots\ldots\ldots\ldots (17)$$

a changes very little with i_o. i_o, i_1 and i_h are connected by the wave equation (14).

$$\tan\frac{1}{4}(\phi-\beta) = c\tan\frac{1}{4}(\phi+\beta) \quad \text{where} \quad c = \frac{r-\rho}{r+\rho} \ldots\ldots (18)$$

As both ϕ and β are very small angles and

$$\frac{1}{2}(\phi+\beta) = 90^\circ - i_h,$$

$$(\phi-\beta) = 2c(90^\circ - i_h) \text{ or } \beta = (1-c)(90^\circ - i_h) \ldots\ldots (19)$$

$$\frac{d\Theta}{di_h} = \text{approximately } \frac{d\beta}{di_h} = c-1 \text{ (in radians)} \ldots\ldots (20)$$

These equations and equation (14) furnish most of the data needed in equation (1). F was taken from Slichter and Gabriel (1933, case 1); log $C = 2.0$, as found from $\bar{P}$. Table V gives the observed values from Table I and calculated values

TABLE V.

Observed values of log u for Py (details as in Table 1) and calculated values, a) for $V = 6.00 + 0.0095\ (h-18)$; b) $V = 6.05 + 0.0019h$; c) $V = 6.05$, constant.

Distance	100	150	200	250	300	350	400	500 km.
Observed	0.5	0.8	0.6	0.5	0.2	0.0	−0.2	−0.5
Calc. a)	0.5	0.6	0.6	0.6	0.6	0.5	0.5	0.5
b)	−0.1	0.0	0.0	0.1	0.1	0.1	0.0	0.0
c)	−0.5	−0.4	−0.4	−0.4	−0.4	−0.4	−0.4	−0.4

for various values of b. The agreement between the observations and the calculated values for a) is good up to a distance of about 300 km. In case a) the deepest point of the ray to 300 km. would be about 20 km. below the bottom of the gran-

itic layer; this is the correct order of magnitude for the thickness of the intermediate layer (15 km. from travel times; Gutenberg, 1944b), and the observed Py-phases to distances of 300 km. and beyond would be diffracted rays. The ray arriving at the surface at $\Delta = 300$ km., would penetrate only about 4 km. into the layer in b) and slightly more than 1 km. in c). Thus, assumption a) fits the data, but we must keep in mind that the amplitudes of *Py* may be noticeably affected by the energy flow near the discontinuity as mentioned above. If we assume that the source is within the granitic layer, the calculated amplitudes are by far too small.

Combining the results, we find that the relatively large amplitudes of *Py* indicate that the source of earthquakes in southern California is usually at the bottom of the granitic layer, as has been found already from the travel times. The velocity of longitudinal waves in the first intermediate layer is given approximately by $V = 6.0 + 0.01\ (h - 18)$ km./sec, where the figure 0.01 gives only the order of magnitude. The corresponding increase in the bulk modulus by roughly 1¼ per cent corresponding to a pressure increase by 1000 atm. is of the order of magnitude observed in experiments.

In southern California, a second intermediate layer (Fig. 1) is indicated by the phases *Pm* and *Sm* (Gutenberg, 1944b). The velocity of longitudinal waves in this layer is about 6.9 km./sec (Table II). Theoretically *Pm* and *Sm* should be smaller in amplitude than the corresponding *Py* and *Sy* waves.

In the preceding discussion of the first two layers the distance Δ^* (Fig. 1) at which the waves begin to decrease rapidly has added valuable information. The thickness of the granitic and first intermediate layers seems to be the same, within the limits of observations, everywhere in southern California and, correspondingly, the amplitudes of $\bar{P}$, *Py* and *Pn* do not depend noticeably on the wave paths (Table I, columns a) and b)). Contrasting with this, the second intermediate layer seems to be much thicker under the mountains than under the lowlands. The maximum, under the Sierra Nevada, is more than 20, perhaps about 30 km., unless there are additional layers, and the minimum probably 5 km. or less under the coastal areas (Gutenberg, 1943a, 1944b). Consequently, it is to be expected that the critical distance Δ^* at which the true *Pm* ends is greater for paths under mountain regions than for waves travelling mainly under lowlands. Of chief importance is the thick-

ness of the second intermediate layer in the central part of the path.

TABLE VI.

Observed values of log u, details as in Table I, for Pm for paths prevailing under a) lowlands, b) mountain regions. n = number of observations.

Δ in km. average		170	205	225	245	260	275	310	370	440
log u	a)	0.6	0.4	0.1	0.1	−0.4	−0.6	−0.8	−0.6	−0.8
	b)	0.8	—	0.5	(0.3)	0.4	−0.1	−0.2	−0.6	−0.7
n	a)	14	4	5	4	4	4	6	4	4
	b)	6	0	3	2	9	4	8	16	6

Table VI confirms the theoretical conclusions. Complications just discussed, make it impossible at present to obtain even approximate results concerning the change of wave velocity with depth.

Pn IN SOUTHERN CALIFORNIA SHOCKS.

Pn forms the beginning of the seismograms at distances beyond about 150 km., depending on the structure above the Mohorovičić discontinuity (See Fig. 1). In addition to the complications mentioned in connection with *Py*, the effects of the refractions across the boundaries of the intermediate layers must be considered. Equations similar to (17), (18), and (19) again hold. Regardless of the number of intermediate layers, the ray equation (14) gives (See Fig. 5)

$$\sin i_4 = m \sin i_h, \text{ where } m = \frac{V_2\, s}{V_3\, r} \quad \ldots\ldots\ldots\ldots\ldots (21)$$

Approximately

$$\frac{d\Theta}{di_h} = \frac{d\beta}{di_h} = (c-1)\frac{m \cos i_h}{\cos i_4} \text{ where } c = \frac{s-\rho}{s+\rho} \quad \ldots\ldots (22)$$

u may now be calculated from (1), in a way similar to the calculation for *Py*, with log $C=2$ as before. The results depend much on the energy loss at the various discontinuities. However, these factors change very little with distance, except for those connected with the passage of the waves through the Mohorovičić discontinuity. Calculations have been made under a wide variety of assumptions as to the layering, the value of b, and also with the supposition that the

faulting proceeds down to the Mohorovičić discontinuity. Except for this last assumption, the calculated values for short distances were too small, depending on the value of *b*. This may be partly an effect of the energy flow near the discontinuity, and it is to be expected larger for *Pn* than for *Py*, if for *Pn* the value of *b* is smaller than for *Py*. In Table VII,

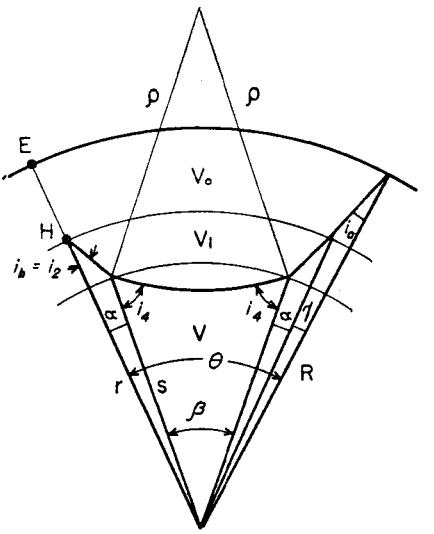

FIG. 5

observed and calculated values are given together. The last three "observed" values are based on 27 records of the short period vertical Beinoff seismograph at Tucson; from comparison with values at shorter distances, it has been found that about 1.1 must be subtracted from the logarithm of the amplitudes to give the results found from the standard horizontal torsion seismographs.

All calculated curves have one property in common—they

TABLE VII.

Observed values of log *u*, details as in Table I, and calculated values for *Pn*, assuming $V = 8.0 + 0.01\ (h - 40)$ km./sec.

Distance	130	200	250	300	350	400	500	600	650	750	850 km.
observed	0.0	0.0	−0.3	−0.5	−0.5	−0.7	−1.0	−1.2	(−1.3)	(−1.5)	(−1.8)
calcul.	−1.1	−0.9	−0.8	−1.8	−0.8	−0.8	−0.7	−0.7	−0.7	−0.7	−0.7

give amplitudes increasing with distance throughout the range for which observations are available (compare Jeffreys, 1937, p. 218). The observations, except for the beginning, show clearly the opposite trend; near 400 km., the amplitudes are about 1/10, and near 800 km. roughly 1/100 of those near 180 km. This fact has been found previously for various regions (see, for example, Gutenberg, 1932, p. 199; Jeffreys, 1937, p. 218). The most reasonable assumption is that our basic equation (3) is incorrect below a depth of about 50 km., because there the increase in velocity is no longer proportional to the depth, but that the rate of increase becomes smaller and smaller with depth, until a depth of roughly 60 or 70 km. the velocity even begins to decrease slowly. The amplitudes of these waves will decrease rather rapidly with distance. Theoretically, they are zero, if the rays have their deepest point at a depth where the velocity decreases downward by only about 0.0013 km./sec per km. If V decreases more rapidly or decreases discontinuously, a "shadow zone" for Pn-waves will result at the earth's surface, in which only diffracted Pn-waves are recorded. As the data for southern California shocks are too scanty for the investigation of this problem in detail, records of Huancayo, Peru, have been examined; the results are discussed in the next section.

THE DEPTH AT WHICH THE MELTING POINT IS REACHED.

One of the most important problems concerning the structure of the earth is to determine the depth (or depths) at which the melting point of the material is reached. It has been discussed by geophysicists, geologists, volcanologists, mineralogists, seismologists (for example, Gutenberg, 1939, p. 161; Daly, 1943, p. 405; Anderson, 1938; Buddington, 1943; Gutenberg and Richter, 1939) but no definite answer has been given, though many agree that a depth of about 80 km. would fit well for this boundary. Such a depth would not disagree with studies on the temperature in the earth and the change of melting point with pressure, would explain the lack of strength below this depth which permits the post glacial uplifts, would agree with the properties of rocks to be expected at this depth, and would explain the peculiar behavior of the velocity V of longitudinal waves which has just been mentioned.

Some details are furnished by a study of the "shadow zone" for P and S. If the focal depth in shallow earthquakes

increases, approaching the critical depth D where the wave velocity is supposed to decrease suddenly (with gradual increase below), the shadow zone moves to shorter epicentral distances (Fig. 6); its inner radius reaches a minimum, if the focus of

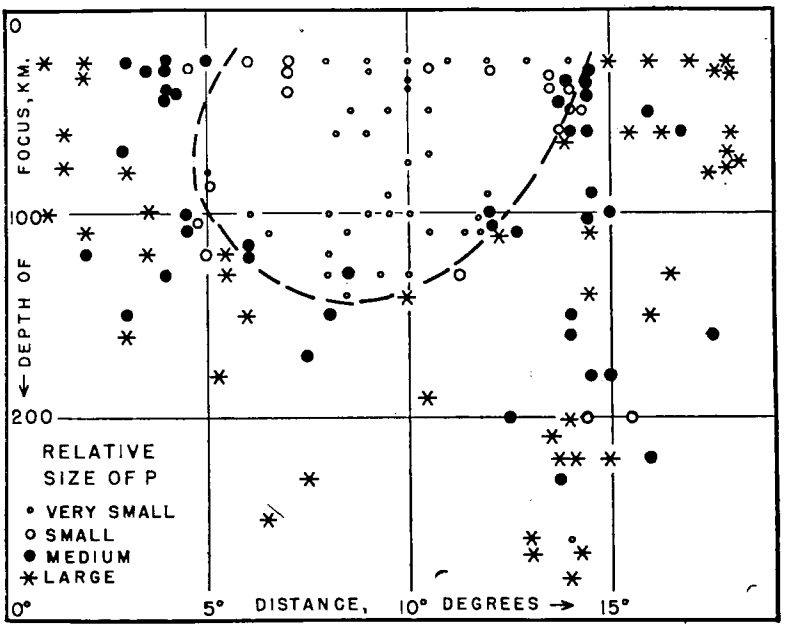

FIG. 6

Fig. 6. Relative amplitudes of P waves recorded at Huancayo, Peru, as a function of epicentral distance and focal depth.

the earthquake is near the critical depth D. If the focal depth increases still more, the width of the shadow zone decreases; the latter disappears, if the source of the shock is below the depth where the wave velocity has increased to approximately the same value as above the depth D in the crystalline material;

TABLE VIII.

Relative amplitudes of P in shocks recorded at Huancayo, Peru.

Date	Hour	Depth of focus, km.	Distance degr.	Amplitudes of P
1933 Aug. 8	23h	170	7½	medium
Sep. 14	8	100	9	very small
Oct. 1	2	120	5½	large
Oct. 10	3	110	11½	very small
Oct. 12	7	100	12	very small

TABLE VIII (Continued).

Relative amplitudes of P in shocks recorded at Huancayo, Peru.

Date	Hour	Depth of focus, km.	Distance degr.	Amplitudes of P
Nov. 3	4	70	10½	very small
Dec. 10	7	60	18	large
1934 Mar. 24	22	270±	14¼	large
Mar. 31	3	60	16¾	medium
1937 Sept. 24	19	130	11¼	small
Oct. 12	20	110	14½	large
1938 Jan. 9	20	120	19	small
Apr. 17	14	60	8¼	very small
Apr. 24	14	180	14½	medium
Aug. 4	8	220	23¾	large
1939 Jan. 18	1	70	18	large
May 13	0	210	14	large
May 19	18	100	9¼	very small
July 4	18	290	13	very large
Sept. 13	18	130	8	very small
Sept. 20	6	60	1½	very large
Oct. 5	4	200	12½	medium
Oct. 7	23	110	8½	very small
Nov. 18	7	40	4	medium
Nov. 26	6	130	4	medium
Dec. 13	18	100	4½	medium
Dec. 24	22	600±	7	medium
1940 Jan. 7	21	100	6	very small
Feb. 12	0	60	15½	very large
Mar. 24	11	280	14	large
Mar. 31	16	50	8½	very small
Apr. 8	8	50	21½	large
May 4	16	30	7	small
May 5	2	40	7	small
Aug. 4	16	130	3½	large
Aug. 7	2	100	12	medium
Aug. 26	2	100	1	very large
Sept. 18	15	110	12	very small
Sept. 23	7	550	16	very large
Sept. 24	9	150	6	large
Oct. 1	10	75	18	large
Oct. 3	4	110	11	very small
Oct. 4	7	75	10	very small
Oct. 6	15	60	9	very small
Oct. 23	2	140	10	large

TABLE VIII—(Continued).

Relative amplitudes of P in shocks recorded at Huancayo, Peru.

	Date	Hour	Depth of focus, km.	Distance degr.	Amplitudes of P
	Oct. 27	10	50	9½	very small
	Nov. 3	6	75	1½	large
	Dec. 4	19	30	2	large
	Dec. 10	0	90	9	very small
	Dec. 22	18	230	7½	very large
1941	Jan. 19	8	40	10	very small
	Jan. 24	5	130	8½	medium
	Jan. 30	4	40	4	medium
	Feb. 2	23	30	18½	medium
	Mar. 10	8	110	2	large
	Apr. 3	14	260	13	large
	Apr. 3	15	260	13	very large
	May 11	5	30	3½	medium
	July 3	7	60	21	very large
	July 10	9	120	8	very small
	July 11	1	30	18	large
	July 11	2	30	18	large
	Aug. 10	19	220	16	medium
	Aug. 14	1	180	15	medium
	Aug. 24	22	110	14½	medium
	Sept. 7	22	30	9	very small
	Oct. 15	0	100	3½	very large
	Oct. 15	9	110	4½	medium
	Nov. 10	9	210	13½	large
	Dec. 14	6	110	4½	small
	Dec. 14	10	70	3	medium
	Dec. 31	17	30	10½	small
1942	Jan. 8	15	110	6½	very small
	Feb. 15	14	150±	8	medium
	Feb. 24	11	200±	21	large
	Mar. 1	17	50	16	medium
	May 17	15	50	14	small
	May 22	10	130	16½	large
	June 6	5	50	14	small
	June 6	10	50	14	small
	June 12	10	50	10½	very small
	June 16	7	60	14	small
	June 16	21	60	14	large
	June 29	6	100	20	large
	July 2	7	40	14	small

TABLE VIII—(Concluded).

Relative amplitudes of P in shocks recorded at Huancayo, Peru.

Date	Hour	Depth of focus, km.	Distance degr.	Amplitudes of P
July 4	0	40	14	very small
July 4	1	40	14½	medium
July 4	4	40	14½	medium
July 4	6	40	14½	medium
July 7	12	30	14½	medium
July 8	6	140	14½	large
July 8	22	60	14½	medium
July 12	5	30	13	small
Aug. 30	19	80	3	very large
Sept. 6	15	60	16½	very large
Sept. 12	5	30	4	medium
Sept. 30	15	80	5	very small
Sept. 30	16	80	5	small
Nov. 6	13	120	6	medium
Nov. 8	10	30	4½	small
Nov. 12	15	40	14	medium
Nov. 12	18	40	13½	small
Nov. 12	22	40	13½	small
Nov. 17	23	40	4	medium
Dec. 1	2	40	10	very small
Dec. 15	9	40	14	medium
Dec. 26	12	50	19	very large

(in Fig. 6 at 140 to 150 km.). Theory, and observations from 38 records at Huancayo, Peru, were discussed by Gutenberg and Richter (1939; with characteristic seismograms).

Table VIII contains additional data; they are plotted in Fig. 6 together with those published previously. The abscissas in Fig. 6 are epicentral distances of the shocks, the ordinates (downward) the depths of the hypocenters (*h* in Fig. 1); the relative intensity of *Pn* (after reduction to the same magnitude of the shock) is indicated by various symbols explained in the figure. The ratio between the "very large" and the "very small" amplitudes is of the order of 100. By far the greater number of the small *Pn*-waves are found in the section of the figure outlined by a barred line.

Figure 6 indicates that the minimum velocity occurs at a depth of not over 100 km.; no exact value can be given, nor is it possible to find the amount of decrease in the velocity in *V* by this method. However, observed travel times indicate that

it cannot exceed a few tenths of 1 km./sec. This decrease may be sudden or gradual over a small depth range (up to about 30 km.) as the shadow zone ends abruptly; it is followed by large amplitudes and does not exist if the hypocenter is below about 140 km. At this depth, the velocity V must have about the same value as at the depth where the decrease begins. For greater depths the increase in velocity remains large enough to be found from travel time observations. All these phenomena are explained by the assumption that the material has its melting point at a depth of about 80 km.

THE AMPLITUDES OF TRANSVERSE WAVES.

Theoretically, the transverse waves can be used in the same way as the longitudinal waves. The fundamental equation (1) remains unchanged, and most of the other equations remain correct. However, there is one additional theoretical difficulty. Whereas the direction of the vibrations in longitudinal waves is given by the angle of incidence, in transverse waves (S-waves) the particles may oscillate in any direction perpendicular to the ray. The amplitudes of S may be given by two components, one purely horizontal ("*SH*"), the other in the plane of the ray, with a horizontal as well as a vertical component ("*SV*"). The ratio SH/SV depends mainly on the mechanism of the shock and may have any value. It enters our problem since the ratio of the refracted and the incident energy at discontinuities, as well as the ratio $(u/A)_0$ of the horizontal ground displacement at the station to the incident amplitude there, are different for *SH* and *SV*. On the other hand, the observations of the amplitudes of S-waves are less accurate than those for P; S is frequently disturbed by surface waves, and the small Sn-waves are superimposed on the tail of the P-group, thus differing from Pn which usually forms the beginning of the seismogram.

The measurements of S were carried out in the same way as those for P. The number of observations is somewhat less than for P. Averages for logarithms of the trace-amplitudes of the four S-phases corresponding to the P-phases in Tables III, V, VI and VII are given in Table IX. The last four lines of this table give the resulting values of log (S/P) for the corresponding pairs of waves. These ratios depend on the change of Poisson's ratio with depth and the values of C, $(u/A)_0$ and of F in equation (1). The average for the loga-

TABLE IX.

Logarithms of average horizontal trace-amplitudes of *S*-waves in Southern California earthquakes of magnitude 5 and of their ratios to the amplitudes of the corresponding *P*-waves. For details see Table I.

Distance	25	50	75	100	150	200	250	300	350	400	450	500 km.
log $\bar{S}$	(2.9)	2.4	2.1	1.9	1.8	1.4	1.2	1.1	0.7	0.6	0.3	0.3
log Sy				1.7	1.5	1.3	1.2	1.0	0.5	0.3	0.2	0.1
log Sm						0.8	0.8	0.5	0.2	0.1		
log Sn					1.2	1.0	0.7	0.3	0.2	0.1	0.0	—0.2
log ($\bar{S}/\bar{P}$)	(0.8)	0.9	0.7	0.7	0.8	0.7	0.6	0.6	0.6	0.6	0.6	(0.8)
log (Sy/Py)				1.2	0.7	0.7	0.7	0.8	0.5	0.5	0.6	(0.8)
log (Sm/Pm)						(0.4)	0.8	1.1	0.9	0.8		
log (Sn/Pn)					1.2	1.0	1.0	0.8	0.7	0.8	0.8	0.9

rithms of the first two is about 0.7, for the third about 0.9. Thus, as an average the recorded amplitudes of $\bar{S}$ and *Sy* are about 5 times those of the corresponding *P*-waves. This is partly a consequence of the fact that the periods in the *S*-waves are sometimes longer than in the *P*-waves, so that the same amplitude in *P* and *S* corresponds to a larger energy in the *P*-waves; also, a given amplitude of *A* of the arriving wave produces a larger horizontal ground movement *u* in the the *S*-waves than in the *P*-waves.

In Table X characteristic values of u/A are given for various distances Δ. Except for distances less than 15 km., $\bar{S}V$ ought to be noticeably smaller than $\bar{S}H$ if both started out with the same amplitudes. This agrees with many observations (Gutenberg, 1943c, Fig. 1). Consequently, we have to compare the values of $(u/A)_0$ for *P* with those for $\bar{S}H$. At distances between 25 and 300 km., their ratio varies between 1.1 and 1.7, the logarithm between about 0.0 and 0.2. Com-

TABLE X.

Values of $(u/A)_0$ as a function of angle of incidence i_0 and corresponding approximate distance Δ(in km.) of $\bar{P}$ and $\bar{S}$.

i_0	0	15	29	32	34	35½	42	45	59	74	79	83°	90°
Δ	0	5	10	11	12	13	16	18	30	60	110	300	—
$\bar{P}$	0.0	0.6	1.1	1.2	1.2	1.3	1.5	1.5	1.7	1.7	1.5	1.2	0.0
$\bar{S}H$	2.0	2.0	2.0	2.0	2.0	2.0	2.0	2.0	2.0	2.0	2.0	2.0	2.0
$\bar{S}V$	2.0	1.9	1.7	1.7	2.0	5.0	0.4	0.0	0.5	0.5	0.4	0.3	0.0

bining the results of Tables IX and X, it follows that the amplitudes of the $\bar{P}$- and $\bar{S}$-waves arriving at distances between about 25 and 300 km. have about the same amplitude ratio. Consequently, the value of the square root in equation (1), which depends on the change of velocity with depth, changes in approximately the same way for $\bar{S}$ and $\bar{P}$. Besides, $\bar{S}$ shows a similar rapid decrease in amplitudes with distances between 300 and 350 km. (Table IX) as $\bar{P}$, indicating the end of the direct waves. Both results lead to the conclusion that in the granitic layer the curvature of the rays must be about the same, Poisson's ratio must be approximately independent of depth, and the change in the rigidity with depth must be of the same order of magnitude as the change in the bulk modulus, as we had assumed in equations (7) to (10).

Similar conclusions may be drawn from the other pairs of waves with regard to the intermediate layers and the material below the Mohorovicic discontinuity although we must keep in mind that sources of error increase with the number of quantities involved. As to *Sy*, $(u/A)_0$ is about 0.5 for *SV*, 2.0 (as always) for *SH*, as compared with 1.6 for *Py*; as to *Sn*, it is near zero for *SV*, 2.0 for *SH*, as against 1.4 for *Pn*. In addition, differences in the loss of energy (*F* in equation 1) at the points of refraction must be considered. From the calculations (for details, see Gutenberg, 1944a) it is evident that for angles of incidence near 90° in the layer with higher velocity, the percentage of energy lost in the refraction is about equal for *P* and *SV*, but that *SH* carries roughly between 1½ and 2 times the energy of *SV* across the discontinuity. The energy lost by *Sn* or *Pn* in passing through the discontinuities between the intermediate layers and into the granitic layer is very small (between a few and about 15 per cent) in all instances, and the differences are negligible. Thus, theoretically we should expect that on the average log (*Sy/Py*) should be about 0.1 greater and log (*Sn/Pn*) about 0.3 greater than log ($\bar{S}/\bar{P}$), if the radius of curvature of the rays and the relative increase in velocity with depth are the same for *P* and *S*. These calculated values correspond very closely to the observations (second part of Table IX). The sudden decrease in amplitudes at a distance of about 300 km. is even more strongly marked in Sy than in Py indicating very closely the same curvature of those rays of *Py* and *Sy* which are grazing at the bottom of the first intermediate layer. Also,

the rapid decrease in *Sn* with distance, especially beyond a distance of about 200 km. corresponds to the change in *Pn*. The Huancayo records show the same behavior for *S* as for *P*, whenever the depth of focus was large enough to prevent surface waves with amplitudes exceeding those of S. All data indicate, that the velocity of *S* below the Mohorocičić discontinuity changes in a way similar to that of *P*.

Values for the rigidity μ in the various layers are given in Table II. They change with depth in each of the layers in a similar proportion as the values for k.

SUMMARY.

An investigation of amplitudes of P-waves in southern California in about 300 instances, having epicentral distances from 5 to 570 km. indicates that the velocity V of longitudinal waves in the granitic layer at depths h (in km.) between about 2 km. and its bottom at about 18 km. is given by $V=5.56+0.001\ h$ km./sec. The second term is a first approximation only and indicates an increase in the bulk modulus by about ¾ per cent corresponding to an increase in pressure by 1000 atm. This is of the same order of magnitude as the values found for granite in laboratory experiments and from the theory of finite strain.

Similarly, the investigation of *Py*-waves gives a velocity of $6.0+0.01\ (h-18)$ km./sec for the (first) intermediate layer and a resulting increase in the bulk modulus by about 1¼ per cent per pressure increase of 1000 atm. Travel times as well as amplitudes lead independently to the conclusion that most of the 50 shocks used originated at the bottom of the granitic layer. In shocks with faulting completely inside the granitic layer only, the amplitudes of *Py* should be about the same size as those of *Pn*.

The fact that the amplitudes of the various *S*-waves change with distance in a similar way as those of the corresponding *P*-waves, indicates that the effect of pressure and temperature on the coefficient of rigidity is relatively the same as on the bulk modulus.

The Mohorovičić discontinuity is at a depth of about 35 to 40 km. in the coastal areas of southern California, but deeper under mountain ranges. The velocity of *Pn* below it is close to 8.0 km./sec. At first, the velocities of both, *P* and *S*, increase with depth, probably at a rate similar to that in the

upper layers, but the rate of increase falls off rapidly with increasing depth, resulting in a rapid decrease of the amplitudes of *Pn* and *Sn* with distance beyond $\Delta = 200$ km. Amplitudes of *Pn* and similarly of *Sn* in intermediate shocks without appreciable surface waves on records of shocks originating at various depth within a radius of about 2000 km. from Huancayo, Peru, and recorded at the station there confirm the previous results of Gutenberg and Richter (1939) concerning the relationship between the epicentral distances at which the amplitudes of *Pn* are very small, and the focal depth of the shocks (See Fig. 6.) These findings can be explained on the assumption that at a depth of about 80 km. the melting point of the material is reached. Immediately above that critical depth, the effect of temperature on the bulk modulus and on the coefficient of rigidity may approach or even surpass the effect of pressure. At the critical depth itself, there may be a slight sudden decrease of the wave velocity. Experimental data (Birch et al., 1942, pp. 15, 28 and 59) are insufficient to decide which decrease is larger at the melting point, that of the elastic constants or that of the density. At greater depth, the effect of the temperature on the bulk modulus and the coefficient of rigidity becomes more and more insignificant. Whereas above the critical depth, a minimum stress of the order of 10^9 dynes/cm.^{2} (the strength), is required to start plastic flow, below this depth the strength is much smaller, and the plastic flow is controlled mainly by the plasticity of the material.

References.

Adams, L. H., and Williamson, E. D.: 1923, The compressibility of minerals and rocks at high pressures, Franklin Inst., Jour., vol. 195, p. 475.

Anderson, E. M.: 1938, Geophysical data applied to the magma problem, Bulletin volcanologique, Ser. 2, Tome 3, pp. 42-82.

Birch, F.: 1938, The effect of pressure upon the elastic parameters of isotropic solids, according to Murnaghan's theory of finite strain, Jour. Applied Physics, vol. 9, pp. 279-288.

————: 1939, The variation of seismic velocities within a simplified earth model in accordance with the theory of finite strain, Seismol. Soc. Amer., Bull., vol. 29, pp. 463-479.

————: 1943, Elasticity of igneous rocks at high temperatures and pressures, Geol. Soc. Amer., Bull., vol. 54, pp. 263-285.

———— and Dow, R. B.: 1936, Compressibility of rocks and glasses at high temperature and pressures: Seismological application, Geol. Soc. Amer., Bull., vol. 47, pp. 1235-1255.

———— et al: 1942, Handbook of physical constants, Geol. Soc. Amer., Special Papers, No. 36.

Buddington, A. F.: 1943, Some petrological concepts and the interior of the earth, Amer. Mineralogist, vol. 28, pp. 119-140.

Daly, R. A.: 1943, Meteorites and an earth model, Geol. Soc. Amer., Bull., vol. 54, pp. 401-456.

Gutenberg, B.: 1932, Handbuch der Geophysik, vol. 4, Berlin.

————: 1939, Internal constitution of the earth, New York and London.

————: 1941, Mechanism of faulting in southern California indicated by seismograms, Seismol. Soc. Amer., Bull., vol. 31, pp. 263-302.

————: 1943a, Earthquakes and structure in southern California, Geol. Soc. Amer., Bull., vol. 54, pp. 499-526.

————: 1943b, Seismological evidence for roots of mountains, Geol. Soc. Amer., Bull., vol. 54, pp. 473-498.

————: 1943c, Travel times of principal P- and S-phases over small distances in southern California, Seismol. Soc. Amer., Bull., vol. 34, pp. 13-32 (1944).

————: 1944a, Energy ratio of reflected and refracted seismic waves, Seismol. Soc. Amer., Bull., vol. 34, pp. 85-102.

————: 1944b, Reflected and minor phases in records of near-by earthquakes in southern California, Seismol. Soc. Amer., Bull., vol. 34, pp. 137-160.

———— and Richter, C. F.: 1931, On supposed discontinuities in the mantle of the earth, Seismol. Soc. Amer., Bull., vol. 21, pp. 216-222.

————: 1939, New evidence for a change in physical conditions at depths near 100 kilometers, Seismol. Soc. Amer., Bull., vol. 29, pp. 531-537.

Jeffreys, H.: 1926, The reflexion and refraction of elastic waves, Monthly Not. R. Astron. Soc., Geophys. Supplem., vol. 1, pp. 321-334.

————: 1937, A further study of near earthquakes, Monthly Not. R. Astron. Soc., Geophys. Supplem., vol. 4, pp. 196-225.

Joos G. and Teltow, J.: 1939, Zur Deutung der Knallwellenausbreitung an der Trennschicht zweier Medien, Physikalische Zeitschrift, vol. 40, pp. 289-293.

Knott, C. G.: 1899, Reflexion and refraction of elastic waves, with seismological applications, Philos. Mag., vol. 48, pp. 64-97.

Muskat, M., and Meres, M. W.: 1940, Reflection and transmission coefficients for plane waves in elastic media, Geophysics, vol. 5, pp. 115-155.

Ott, H.: 1942, Reflexion und Brechung von Kugelwellen, Annalen der Physik, (5), vol. 41, pp. 443-466.

Richter, C. F.: 1935, An instrumental earthquake magnitude scale, Seismol. Soc. Amer., Bull., vol. 25, pp. 1-32.

Schmidt, O. von: 1938, Ueber Knallwellenausbreitung in Flüssigkeiten und festen Körpern, Zeitschrift f. Techn. Physik, vol. 12, pp. 554-560.

————: 1939, Ueber Kopfwellen in der Seismik, Zeitschrift f. Geophysik, vol. 15, pp. 141-148.

Slichter, L. B. and Gabriel, V. G.: 1933, Studies in reflected seismic waves, Gerlands Beitr. z. Geophysik, vol. 38, pp. 228-238.

Zöppritz, K.: 1912, Ueber die Amplitude der sogenannten ersten Vorläufer in Erdbebendiagrammen und über einige Beobachtungen an Erdbebenwellen, Ges. d. Wissensch. Göttingen, Nachr., Math.-phys. Kl., pp. 123-143.

California Institute of Technology,
Pasadena, California.

(Balch Graduate School of the Geological Sciences, contribution no. 362.)